www.czasopisma.pan.pl PAN POLSKA AKADEMIA NAUK www.journals.pan.pl

Arch. Metall. Mater. **62** (2017), 2B, 1099-1104

DOI: 10.1515/amm-2017-0159

YONG HWAN KIM*, JEONG- JUNG OAK**, KI- CHANG BAE*, WOOK JIN LEE***, YONG HO PARK*,****#

HIGH-TEMPERATURE OXIDATION BEHAVIOR AND KINETICS OF FORGED 12Cr-MoVW STEEL

The oxidation kinetics of forged 12Cr-MoVW steel was investigated in an air (N_2+O_2) atmosphere at 873-1073 K (Δ50 K) using thermogravimetric analysis. The oxidized samples were characterized using X-ray diffraction, and the surface and cross-sectional morphologies were examined using scanning electron microscopy coupled with energy-dispersive X-ray spectroscopy. The forged 12Cr-MoVW steel samples exhibited parabolic behavior and a low oxidation rate compared with their as-cast counterparts. A protective oxide layer was uniformly formed at relatively low temperature (≤973 K) for the forged samples, which thus exhibited better oxidation resistance than the as-cast ones. These oxides are considered solid-solution compounds such as $(Fe, Cr)_2O_3$.

Keywords: ferritic/martensitic stainless steels, 12Cr-MoVW steel, forging, oxidation kinetics, oxide layer

1. Introduction

Since ultra-supercritical (USC) plants were introduced in the late 1990s, ferritic/martensitic stainless steels have been used as structural materials for components in gas turbines and thermal power plants. These steels have also been used for the rotors, casing valves, tubes, and pipes of USC turbines because of their excellent mechanical and high-temperature creep properties and better price competitiveness compared with austenitic stainless steel [1,2].

The maximum service temperature of these steels is estimated to be approximately 893 K. For components that require oxidation/corrosion resistance at high temperature, 12% Cr steels have been primarily used because they provide better oxidation resistance than 9% Cr steels [3-5]. As superior mechanical and creep properties are required for 500-MW USC facilities of medium-to-large size with extreme operating temperature (866 K) and pressure (25 MPa), the 12% Cr steels used in supercritical (SC) plants have been modified by adding various alloying elements. One of the commercially available alloys in this class of steels is 12Cr-MoVW steel [5]. This alloy was developed by adding Mo, V, and W to AISI 410 stainless steel to increase the creep rupture strength [1,6,7].

However, 12% Cr steels are difficult to forge because of the high content of alloy elements. A processing technique using a dynamic material model is used to optimize the workability and to evaluate the thermal deformation mechanisms of a wide range of metal materials [8-10]. To date, many studies [11-13] have focused on the heat-treatment process, mechanical properties, fracture mechanism, and fatigue of 12% Cr steels; however, the oxidation behavior after hot deformation has drawn little attention.

The present research was aimed at elucidating the effect of hot forging on the oxidation characteristics of 12Cr-MoVW steel. Special emphasis was placed on a detailed examination of the oxide scale to understand the kinetics of and role of the structure in determining the oxidation rate.

2. Experimental methods

The chemical composition of the 12Cr-MoVW steel used in this study (B50A951A1, SeAh Special Steel Corp., Korea) is listed in Table 1. The as-received specimens were normalized at 1313 K for 3 h, quenched in oil, and then tempered at 953 K for 7 h. The heat-treated (as-cast) samples were homogenized at 1373 K for 3 h and finally hot forged to achieve 35% reduction of area. Optical micrographs (OM) of the starting microstructures of the as-cast and forged samples are shown in Fig. 1.

TABLE 1

Chemical composition (wt. %) of the investigated steel

Chemical composition (wt. %)										
C	**Si**	**Mn**	**P**	**S**	**Ni**	**Cr**	**Mo**	**Cu**	**V**	**W**
.205	.266	.775	.0185	.0018	.661	11.650	1.078	.156	.255	1.050

* DEPARTMENT OF MATERIALS SCIENCE AND ENGINEERING, PUSAN NATIONAL UNIVERSITY, BUSAN, REPUBLIC OF KOREA
** MATERIAL ANALYSIS LABORATORY, DEA-IL CORPORATION, ULSAN, REPUBLIC OF KOREA
*** KOREA INSTITUTE OF INDUSTRIAL TECHNOLOGY, BUSAN, REPUBLIC OF KOREA
**** SOCIAL ENTERPRISE, PUSAN NATIONAL UNIVERSITY, BUSAN, REPUBLIC OF KOREA
# Corresponding author: yhpark@pusan.ac.kr

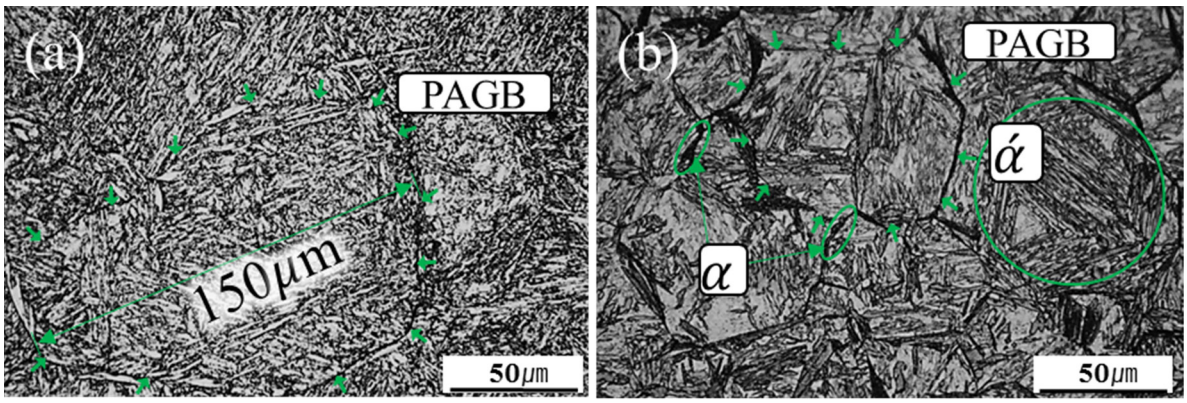

Fig. 1. Optical micrographs of as-cast (a) and forged (b) 12Cr-MoVW steel used in this investigation

For the oxidation test, the specimens were cut into cubes with dimensions of 2.5×2.5×2.5 mm^3. All the specimens were ground using 2400# SiC paper and ultrasonically cleaned in distilled water and ethanol for 10 min before being weighed. Isothermal oxidation experiments at 873-1073 K (Δ50 K) for 60 h were performed using thermogravimetric analysis (TGA, TG/DTA 7300, Seiko, Japan) in an air (N_2+O_2) atmosphere. The heating rate was 10 K/min for all the specimens. The oxide phases were identified using X-ray diffraction (XRD, Rigaku Ultima IV, Japan). The surface and cross-sectional morphologies of the oxidized samples were characterized using field-emission scanning electron microscopy (FE-SEM, TESCAN MIRA 3, Czech Republic) coupled with energy-dispersive X-ray spectroscopy (EDS) operating in back-scattered electron (BSE) mode.

3. Results and discussion

The oxidation rates of the as-cast and forged 12Cr-MoVW steel in the temperature range of 873-1073 K are plotted in Fig. 2, clearly demonstrating the temperature-dependent oxidation kinetics. The oxidation kinetics were evaluated using the

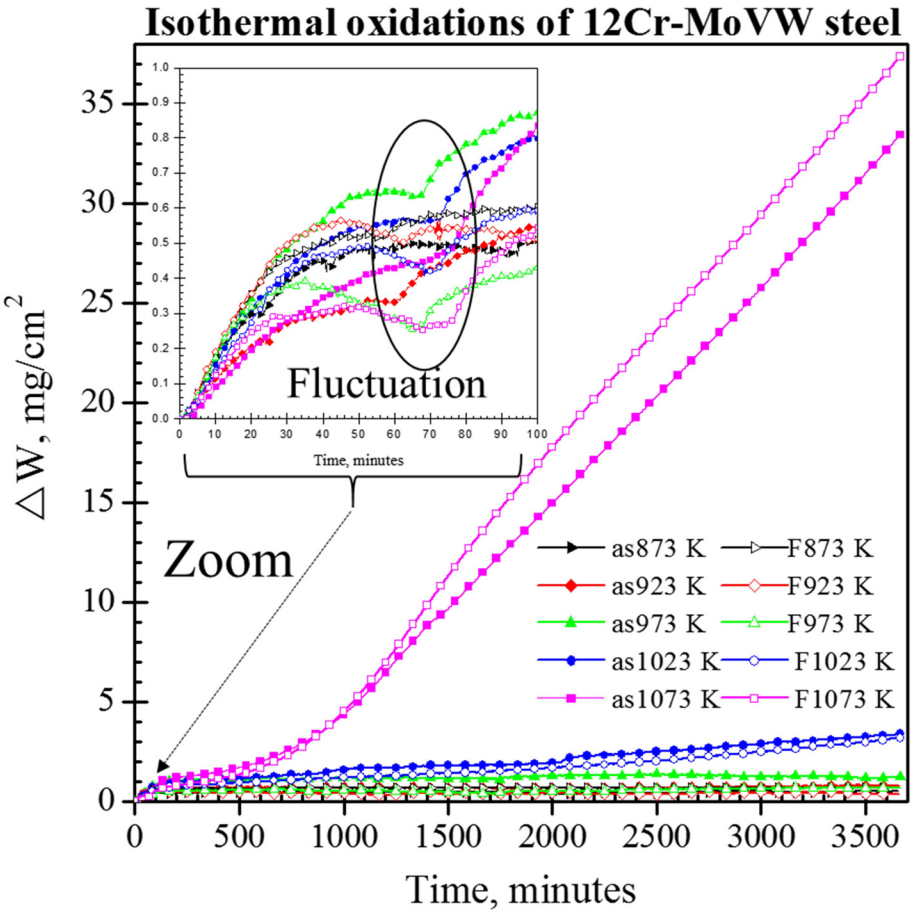

Fig. 2. ΔW versus time curves for the as-cast and forged materials exposed to air at 873-1073 K (Δ50 K) for 60 h (as: as-cast; F: forged)

parabolic rate law $(\Delta W/A)^2 = k_p \cdot t$, where $(\Delta W/A)$ is the weight gain (g/cm^2), k_p is the parabolic rate constant (g^2/cm$^4 \cdot$ min^{-1}), and t is the oxidation time (min) [14,15]. The ΔW and k_P values are summarized in Table 2. The overall oxidation rates of the as-cast specimens are much higher than the forged ones.

The oxidation characteristics between 873 K and 973 K indicate parabolic behavior and low oxidation rates with no measurable increase. The enlarged inset in Fig. 2 shows the initial slope of the curves, where fluctuations of ΔW in the forged specimens are observed at intermediate temperatures between the heating and isothermal temperatures. This phenomenon is attributed to the martensite phase formed in the forged specimens.

At high temperature (>973 K), linear behavior at the beginning with a "breakaway" model [16] is observed in both the as-cast and forged specimens after certain incubation times. The incubation time decreased as the oxidation temperature increased

TABLE 2

ΔW and k_P for each isothermal oxidation in air at 873-1073 K for 60 h and activation energy from Arrhenius plot of k_P for oxidation of the as-cast and forged 12Cr-MoVW steel specimens

Sample	ΔW (mg/cm^2)	K_P (g$^2 \cdot$ cm^{-4}s^{-1})	Q (oxid.) (KJ/mol)
As873 K	0.5411	1.6E-13	
As923 K	0.8060	7.9E-13	
As973 K	1.2282	3.1E-12	379
As1023 K	3.4100	4.9E-11	
As1073 K	33.5800	4.9E-09	
F873 K	0.6833	2.7E-13	
F923 K	0.3812	1.7E-13	
F973 K	0.6721	9.8E-13	387
F1023 K	3.2103	4E-11	
F1073 K	37.4716	6.3E-09	

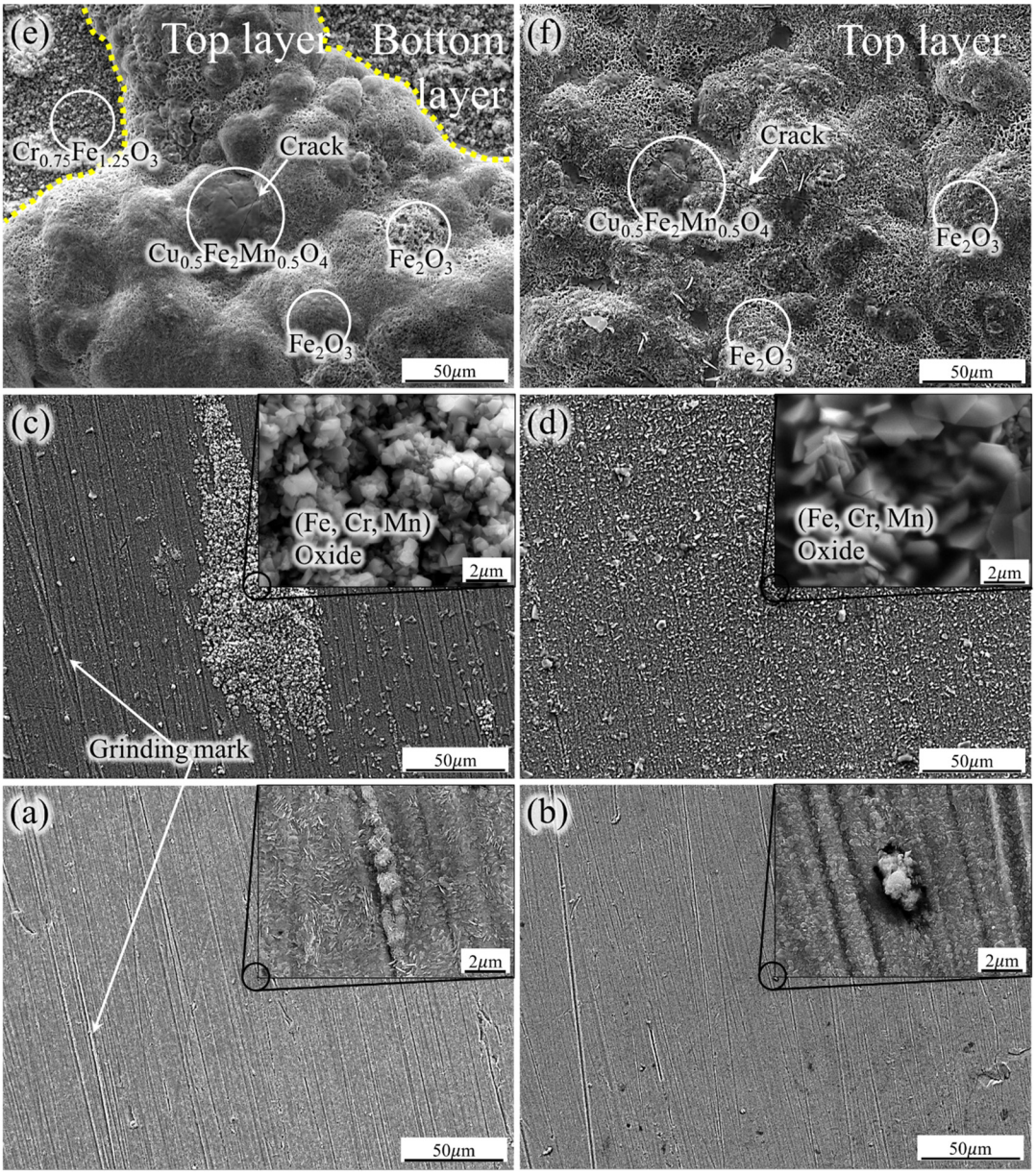

Fig. 3. SEM micrographs of surface morphology of the oxide scales after oxidation in air for 60 h at 873 K (a), 973 K (c), and 1073 K (e) for the as-cast 12Cr-MoVW steel and 873 K (b), 973 K (d), and 1073 K (f) for the forged 12Cr-MoVW steel

from approximately 900 min at 1023 K to 2200 min at 1073 K. The oxidation rates increased continuously with oxidation time.

The activation energy for the forged specimens was calculated to be 387 kJ/mol from an Arrhenius plot of the parabolic constants determined from 873 to 1073 K, as listed in Table 2.

Fig. 3 presents SEM images of the surface morphology of the oxide scales formed on the as-cast and forged materials exposed to air at 873-1073 K for 60 h. The surface morphology of the specimens in air after 60 h depended on temperature, consistent with the oxidation kinetics. As observed in Figs. 3(a-d), at relatively low temperature (≤973 K), a flat and thin oxide scale (≤2 μm) formed that could not cover the grooves resulting from grinding. The oxides formed on the as-cast specimens shown in Fig. 3(c) are observed to be preferentially parallel to the grinding marks, whereas those formed on the forged specimens in Fig. 3(d) are uniformly dispersed. It can be considered that the microstructure of the forged specimens increased the diffusivity of oxygen in the substrate. The oxide nodules formed at 973 K mostly consisted of (Fe, Cr, Mn) oxides in both the as-cast and forged specimens. The XRD patterns in Fig. 4 identify the oxides as (Mn, Fe)(V, Cr)$_2$O$_4$. Identification of the oxide compound of Fe, Cr and Mn is complex because these oxides have similar crystal structures and lattice parameters [17,18]. Most of the oxide compounds were Mn-Cr and Fe-Cr oxides.

At very high temperature (1073 K), the surface was completely covered by oxide nodules in both the as-cast and forged states. The morphology of Fe_2O_3 (hematite) predominantly observed in Figs. 3(e-f) indicates that the specimens are covered by porous oxides. The oxide layers in the as-cast state are divided into two layers. The bottom layer in Fig. 3(e) is a flat oxide scale (Fe-Cr oxide) and corresponds to a corundum-type oxide, $Cr_{0.75}Fe_{1.25}O_3$, according to the XRD results in Fig. 4(a). The top layer in Fig. 3(e) is mainly composed of Fe_2O_3 and a small amount of $Cu_{0.5}Fe_2Mn_{0.5}O_4$. Based on these results, it appears that the oxidation continuously progressed non-protectively by propagating along the cracks of $Cu_{0.5}Fe_2Mn_{0.5}O_4$. Unlike the as-cast specimens oxidized at 1073 K, the forged ones in Fig. 3(f) only consisted of one layer of Fe_2O_3 and $Cu_{0.5}Fe_2Mn_{0.5}O_4$ (the top layer in the as-cast state), indicating that the non-protective behavior was promoted even more than in the as-cast specimens. This finding corresponds well with the higher ΔW values of the forged specimens due to the breakaway oxidation. The oxidation resistance of heat-resistant steels primarily relies on the amount of Cr content. Cr forms a protective oxides which are carried out as a barrier to the breakaway behavior. At 1073 K, it can be proposed that a method of adding Cr originally help the oxidation resistance avoid the breakaway behavior by migrating the cationic Cr atoms from the substrate. In addition, making ultrafine grains near surface are thought to improve the oxidation resistance by producing the abundant grain boundary density.

Figs. 5(a-d) present cross-sectional BSE images of the samples at 873-1073 K, revealing the temperature dependence of the morphologies; the corresponding EDS line scans are presented in Fig. 6. An extremely thin protective oxide scale formed at 873 K, as observed in Figs. 5(a-b), indicating that both the as-cast

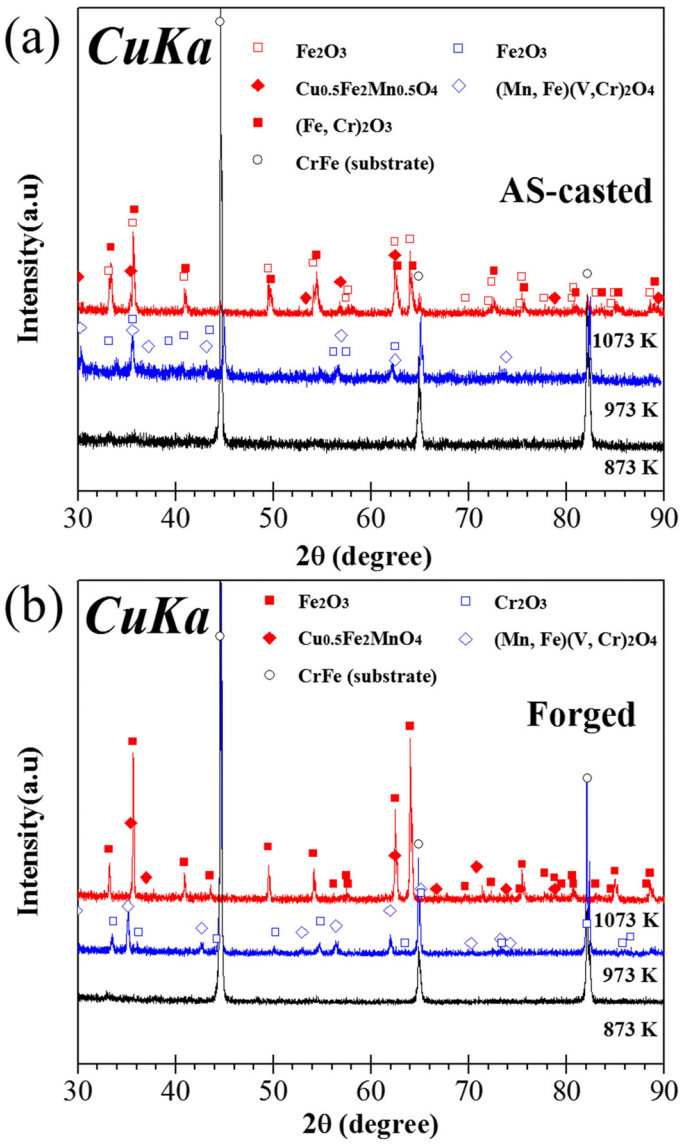

Fig. 4. XRD patterns of the oxide scales formed on the as-cast (a) and forged (b) 12Cr–MoVW steel at 873–1073 K for 60 h in air

and forged specimens were barely oxidized. The oxide layers at 973 K in Figs. 5(c-d) are thicker and mainly consisted of (Cr, Mn) oxides. The solid-solution compounds such as (Fe, Cr)$_2$O$_3$ observed in the forged specimens oxidized at 973 K are considered to have formed because of solidification between the Cr_2O_3 and Fe_2O_3 identified in Fig. 4(b) because these compounds are soluble in each other. At very high temperature (1073 K), the oxide layers in both the as-cast and forged specimens consisted of two layers, with thicknesses greater than 50 μm, as observed in Figs. 5(e-f).

This result indicates that the weak CrFe peaks in Fig. 4 for the sample oxidized at 1073 K originate from the thick oxide layer, which can absorb the X-ray signal from the substrate. Voids are also observed in the outer layer, which included Fe-rich oxide. The EDS line scans through the two layers in Figs. 6(e-f) indicate that the outer layer consisted of Fe-rich oxides, whereas the inner layer mainly consisted of (Fe, Cr, Mn) oxides. Segrega-

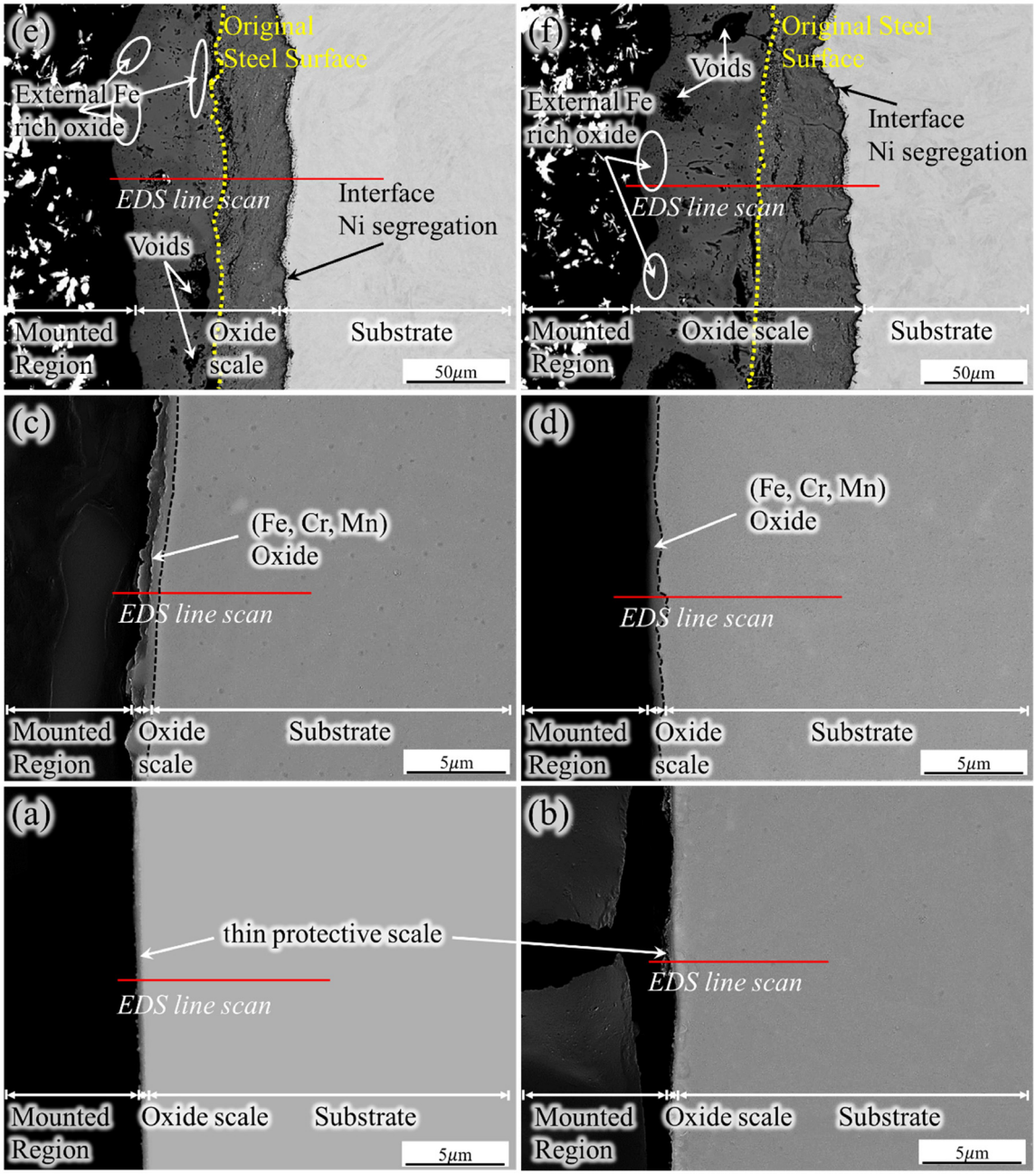

Fig. 5. Cross-sectional BSE micrographs of oxide scales oxidized in air for 60 h at 873 K (a), 973 K (c), and 1073 K (e) for the as-cast 12Cr-MoVW steel and 873 K (b), 973 K (d), and 1073 K (f) for the forged 12Cr-MoVW steel

tion of Ni near the interface between the inner oxide layer and substrate was observed in the EDS analysis, which indicates that the small black dots near the interface in Fig. 5 are due to the Ni segregation.

4. Conclusion

Based on the experimental results, the following conclusions can be drawn:

1. At low temperature (≤973 K), the forged 12Cr-MoVW steel specimens exhibited extremely parabolic behavior and low oxidation rates; in contrast, at high temperature (>973 K), both the as-cast and forged 12Cr-MoVW steel specimens exhibited breakaway behavior.
2. The fluctuation phenomenon of the initial slope of the curves of the forged 12Cr-MoVW steel specimens is thought to be associated with the martensite phase.
3. The oxides of the forged 12Cr-MoVW steel specimens formed at 973 K were uniformly dispersed compared with those of the as-cast state; the protective oxides are considered to be solid-solution compounds such as $(Fe, Cr)_2O_3$.
4. At high temperature (1073 K), both the as-cast and forged 12Cr-MoVW steel specimens formed thick double oxide layers (>50 μm) consisting of hematite and magnetite from the oxide/air interface to the oxide/substrate interface.

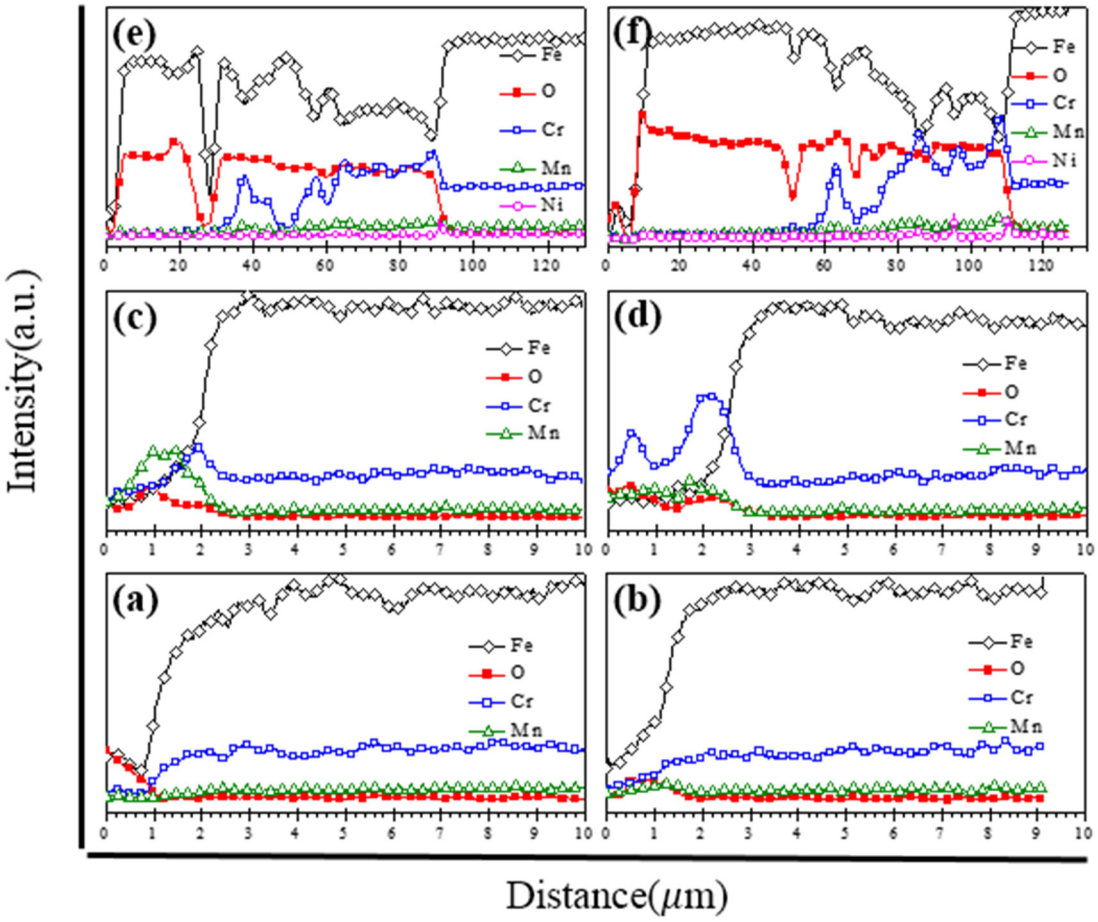

Fig. 6. EDS elemental analysis of the cross-sections in Fig. 5 after oxidation for 60 h in air at 873 K (a), 973 K (c), and 1073 K (e) for as-cast 12Cr-MoVW steel and 873 K (b), 973 K (d), and 1073 K (f) for forged 12Cr-MoVW steel

Acknowledgements

This work was supported by BK21PLUS, Social Enterprise Specialist Development Group.

REFERENCES

[1] R. Viswanathan, J. Nutting, Advanced Heat Resistant Steels for Power Generation, New York, 1999

[2] L. Jong-Pil, H. Ji-Hyun, P. Dong-Kyu, A. In-Shup, J. Korean Powder Metall. Inst. **22**, 52-59 (2015).

[3] R. Viswanathan, W. Bakker, J. Mater. Eng. Perform. **10**, 81-95 (2001).

[4] R. Viswanathan, J.F. Henry, J. Tanzosh, G. Stanko, J. Shingledecker, B. Vitalis, R. Purgert, J. Mater. Eng. Perform. **14**, 281-292 (2005).

[5] M. Fujimitsu, ISIJ INT **41**, 612-625 (2001).

[6] T. Sourmail, Mater. Sci. Tech. Lond. **17**, 1-14 (2001).

[7] T. Fujita, ISIJ INT **32**, 175-181 (1992).

[8] T. Maki, K. Akasaka, K. Okuno, I. Tamura, ISIJ INT **22**, 253-261 (1982).

[9] A. Dehghan-Manshadi, P.D. Hodgson, J. Mater. Sci. **43**, 6272-6277 (2008).

[10] W. Jei-Pil, L. Dong-Won, Y. Jung-Yeul, S. Shun-Myung, K. In--Soo, J. Korean Powder Metall. Inst. **20**, 174-179 (2013).

[11] A.A. Tchizhik, T.A. Tchizhik, J. Mater. Process Tech. **77**, 226-232 (1998).

[12] J. Ha, M. Tabuchi, H. Hongo, A. Toshimitsu Yokobori Jr, A. Fuji, Int. J. Pres. Ves. Pip. **81**, 401-407 (2004).

[13] J. Das, S.M. Sivakumar, Eng. Fail Anal. **7**, 347-358 (2000).

[14] B. Pieraggi, Oxid. Met. **27**, 177-185 (1987).

[15] M. Levy, P. Farrell, F. Pettit, Corrosion **42**, 708-717 (1986).

[16] J.R. Davis, ASM specialty handbook;heat-resistant materials, Cleveland, 1997.

[17] M.J. Graham, Corros. Sci. **37**, 1377-1397 (1995).

[18] M.J. Graham, R.J. Hussey, Oxid. Met. **44**, 339-374 (1995).